WIDEBAND HIGH-POWER TRANSMISSION LINE PULSE TRANSFORMERS

A THESIS IN
ELECTRICAL ENGINEERING

Presented to the faculty of the University of Missouri-Kansas City in partial fulfillment of the requirements for the degree

MASTER OF SCIENCE
in
ELECTRICAL ENGINEERING

By
JAMES KOVARIK

B.A. Rockhurst University, 2019

WIDEBAND HIGH-POWER TRANSMISSION LINE PULSE TRANSFORMERS

James Casper Kovarik, Candidate for Master of Science Degree

University of Missouri-Kansas City, 2021

ABSTRACT

Geometric transformers are often used in radar and communications systems to transition between signal driving and radiating elements that terminate in significantly different geometries with unity input/output impedance. This work demonstrates the design and construction process of a geometric transformer with comparison to simulation and prior art. The focus of this work is on the design, optimization, build and test results of a novel geometric transformer capable of transmitting kilovolt 100-picosecond pulses from a parallel plate geometry into a coaxial geometry, modeled after a transverse electromagnetic (TEM) cell. The transformer operates on a wide frequency bandwidth (.5-2 GHz) with minimal reflection or radiative loss (>1.5 dB loss across the frequency range for both in testing). Further, this work touches on a future project that faces similar challenges under different requirements, and describes how these projects compare in design, production, and outcome.

APPROVAL PAGE

The faculty listed below, appointed by the Dean of the School of Computing and Engineering, have examined a thesis titled “Wideband High-Power Transmission Line Pulse Transformers” presented by James Casper Kovarik, candidate for the Master of Science degree, and certify that in their opinion it is worthy of acceptance.

Supervisory Committee

Anthony Caruso, Ph.D.
Department of Physics and Astronomy

Roy Allen, Ph.D.
Department of Physics and Astronomy

Kalyan Durbhakula, Ph.D.
Department of Physics and Astronomy

CONTENTS

ILLUSTRATIONS

Figure Page

TABLES

ACKNOWLEDGEMENTS

The authors wish to thank the Office of Naval Research for their support under award N00014-17-1-3016.

CHAPTER 1
INTRODUCTION

Geometric unity-gain impedance matching transformers are used in electromagnetic (EM) signal transmission applications in which the signal driving elements and radiating elements are significantly different in physical cross section but terminate with the same impedance. An unconventional shape of mating surfaces is often the case in novel designs within rapidly evolving fields such as radar [1], amplifiers [2], and communications [3] where commercial coaxial terminations are not used. The incongruity of surface geometries necessitates the development of a geometric transformer, which transfers RF power from one cross-sectional geometry to another, with minimal losses and reflections.

In the case of phased ultrashort pulse EM power transmission, it is imperative that a transformer operate on an ultra-wide bandwidth that contains the frequency content of the transmitted pulse, generally in the Gigahertz range. If the transformer is not sufficiently ultra-wideband, the frequency content and wave-shape of the transmitted pulse can be distorted (i.e., 100's of MHz of dispersion). Distortion of the pulse can result in delayed rise and fall times, pulse overshoot, or reverse pulses. In circumstances in which the purpose of the pulse is not only power transmission but also to activate the receiving end on carefully

timed intervals (i.e. 10's of picosecond pulses), distortion of the pulse shape could lead to malfunction of the system. For example, an inadequate geometric pulse transformer in use as a part of a radar could negatively affect the precision and range of the radar.

This is a major consideration in the field of phased array scanning. A phased antenna array operates by combining the transmitted signals of multiple antennae with the correct phase relationship to result in a combined signal that transmits in a desired direction (figure 1) [4]. Each antenna is stimulated by a

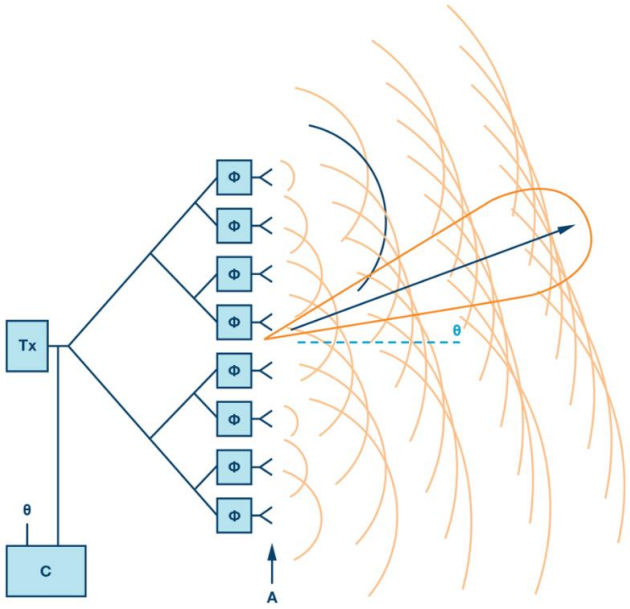

Figure 1. Demonstration of antennas transmitting phased signals that combine into a larger signal that is angled away from the norm.

repeating pulse, and the time delay difference that each antenna receives this pulse is known as the phase of that pulse. The array operates on the principle that the radio waves of separate antenna operating on different phases will combine in certain directions and cancel out or suppress each other in other directions. By adjusting the phase, the direction of the combined signal can be adjusted without the need to mechanically move the array to scan an area. Phased array antennae are common in fields such as radar, to steer a beam quickly across the sky to detect foreign objects [5]. High range radar antennae can be quite large and bulky, so this method was developed as an alternative to steering a dish mechanically, which is significantly slower and prone to hardware breakdowns [6].

If these arrays are to become more powerful and precise, the antennae must be fed with exceedingly high power and high frequency pulses. Higher power kilovolt pulses can increase range and width of the beam, allowing a larger area to be scanned at once. Increasing the frequency of the pulses (e.g. delay of 10's of picoseconds), by increasing the frequencies of the component wavelengths within the pulse, as well as allowing more pulses to be received in the same period, allows the radar array to scan different areas more quickly.

The mechanism to feed the antennae these pulses must do so without affecting the potency or operation of the array. More advanced radar arrays are more demanding of high-power, high-frequency pulses. Unique or novel methods of creating and distributing these high-power, high-frequency pulses may be

restricted to certain transmission geometries and require a geometric transformer to transmit into the components of the array that maintains the intended high-frequency pulses.

1.1 Design Objectives

An antenna array is being designed that includes a novel method of forming the pulses that stimulate the individual antenna elements according to the correct phase. This novel method is a pulse forming transmission line and is used to form very quick and short pulses. The output element of this pulse forming transmission line is a parallel plate. However, the input element to the antenna must be coaxial. Therefore, a geometric transformer must be created to transfer this pulse.

The specific design objectives are to create a high-power transition between the output of parallel plate radiating element and the coaxial input of a low gain UHF antenna element. Each component is to operate in a 4 x 4 array with $\lambda/2$ proximity. The parallel plate output of the radiating element is 1.82cm tall and feed the pulse with a microstrip 4-cm wide. The coaxial input's inner cross-sectional dimensions are a1=3-mm, a2 = 7.75-mm. The resulting characteristic impedance for both input and output are 50-Ω. The maximum voltage handling capacity must be above 10-kV from a <100-ps pulse.

The transmission of the component must fit the following criteria:

- Transmission should be below 1.5-dB power loss, or S21 > .9;
- Wave shape, amplitude, and spectral content across 500-MHz to 2-GHz band should be maintained.

1.2 Survey of Transformer Types

The objective of transitioning between transmission lines, be they waveguide, coaxial, parallel plate, etc., has been extensively studied in the past. Here we will take a survey of several geometric transformer types that have been approached in the past and how they apply to the problem established in this thesis.

A common geometric transformer type is the coaxial-to-waveguide transition [7,8]. These designs often use a probe that extends from the coaxial element and intersects perpendicularly with the waveguide [9,10]. The goal in these transformers is to create a transformation of the TEM mode of electric field that exists in the coaxial into the TE mode within the waveguide, with minimal return losses [11]. In examples such as the probe connection, the transformer usually is designed so the coaxial is the exciting element. As most of these transformer designs are reciprocal networks, the same design can be used to have the waveguide excite the coaxial [12]. These designs are frequently not applicable for high bandwidth purposes. As the placement of the probe is dependent on the wavelength of the transmitted frequency, geometric transformers that utilize a

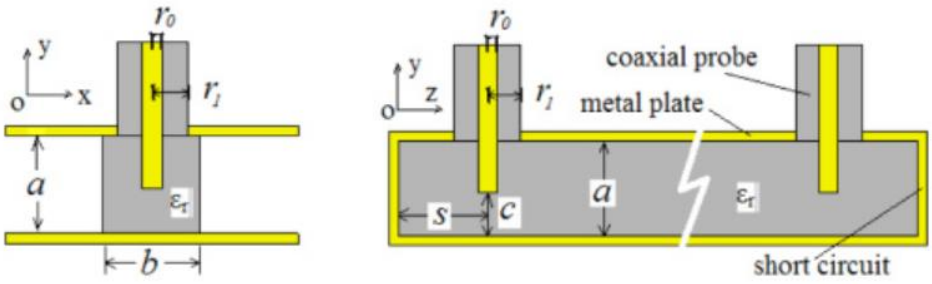

Figure 2. single and multiple probe geometric transformer designs

probe generally only operate on a short bandwidth. Some designs expand the bandwidth by introducing multiple probes from multiple coaxial inputs (figure 2) [13]. However, in doing so, these designs are no longer reciprocal networks, and cannot be used to excite the coaxial element with the parallel plate element.

A wider bandwidth can be achieved by way of a transmission line transformer. These designs connect both elements in parallel, as opposed to the perpendicular connection of the probe, which allows for a gradual change in geometry. In transmission line transformers, there are two major design philosophies. One philosophy introduces a multistep design, in which the impedance is flat except to when jumping to another step (figure 3) [14]. Each step is the length of the quarter wavelength of the central frequency to be transmitted. The bandwidth of the transformer is determined by the number of steps used between elements [15]. However, these designs cannot create the proper geometric transformation to connect with a coaxial element. While the stepped

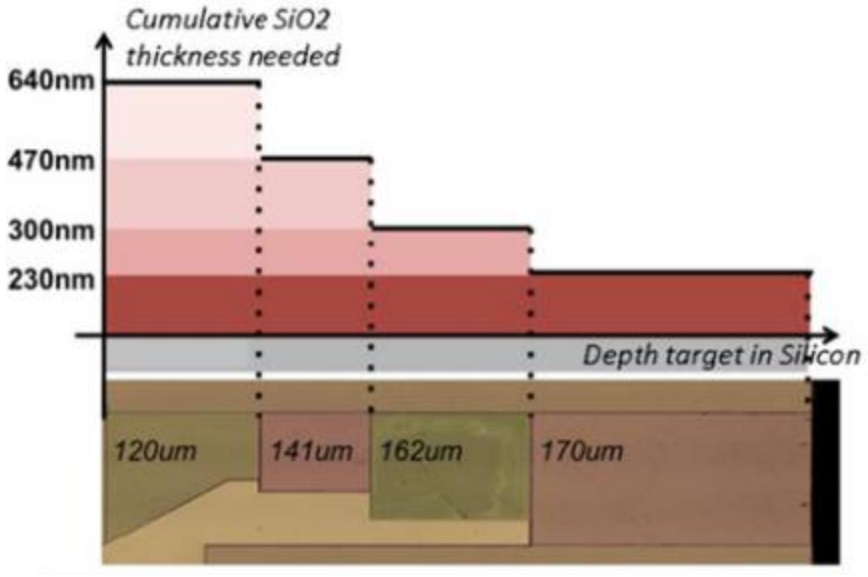

Figure 3. Demonstration of step design for microstrips

design is capable of a high bandwidth [16], this form of transformer is not applicable for our purposes.

Another design philosophy creates a tapered plane, in which the geometry and impedance gradually changes with the length of the transformer (figure 4) [17]. Tapered transformers are also capable of high bandwidth, although they are commonly larger than stepped transformers. These transformer types are more effective at higher frequencies, as their transmission is similar to a high pass filter [17,18]. These designs are also capable of providing a balanced feed and perform with minimal sidelobes, making them optimal for antenna arrays [19]. The active plane on the transformer can take the form of several geometries, from as simple

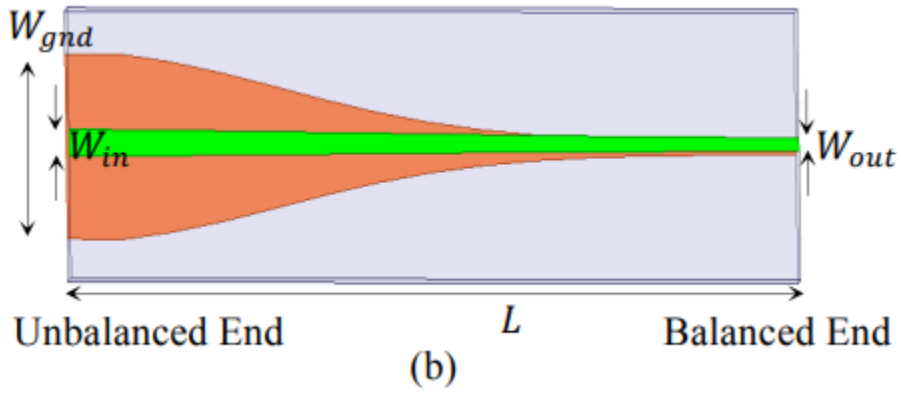

Figure 4. Tapered transmission line balun transformer

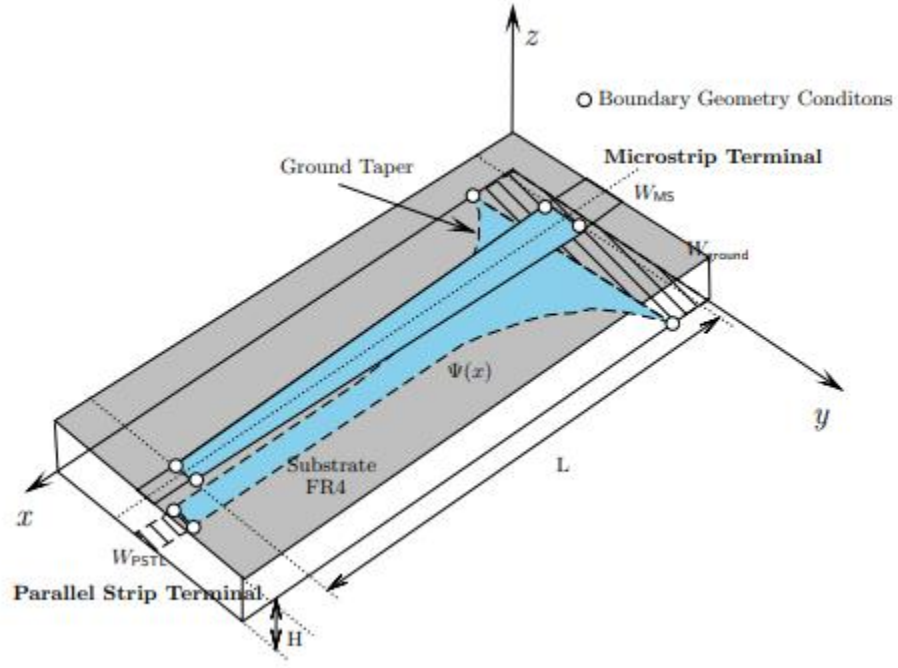

Figure 5. Heckin-taper microstrip design

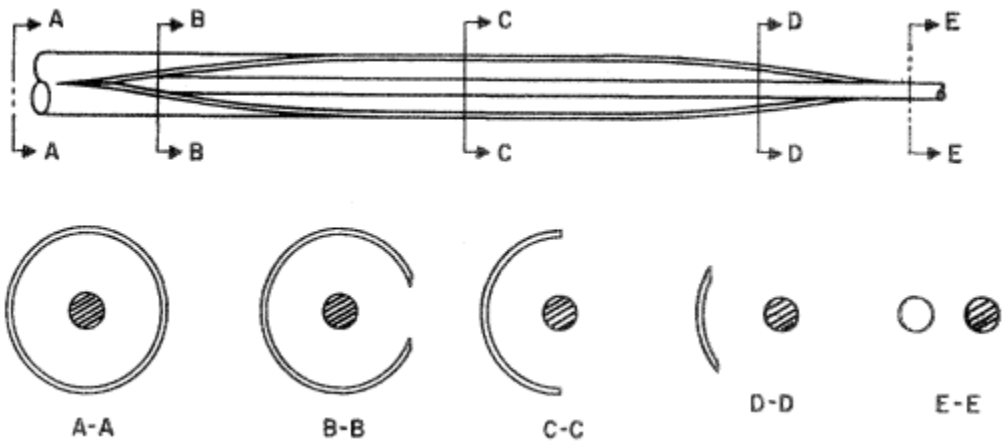

Figure 6. Tchebycheff tapered balun transformer

as a linear taper, to curved geometries such as the Hecken-taper microstrip design (figure 5) [20]. Different designs give different benefits, such as low return losses, higher bandwidth, or preventing fringing fields and mutual coupling. With the tapered plane design, attempting to connect one end to a coaxial element is possible but can create unwanted fringing fields. Modifications must be made to these designs to allow a proper connection with the coaxial element.

It has been attempted before to combine the benefits of the geometric probe transformer, which allows for clean connection between coaxial and parallel plate elements, and the tapered transmission line transformer, which possesses an ultra-wide bandwidth and is applicable in arrays. The Tchebycheff tapered balun transformer (figure 6), for example, connects a coaxial element to

a two-conductor line element with an ultra-wide bandwidth [21]. This transformer does so with little fringing fields and can be used in an array function with no mutual coupling. The Tchebycheff tapered balun transformer does have notable drawbacks, being very large in size, and quite difficult to manufacture. The Tchebycheff tapered balun transformer was a considered design for this project that was ultimately decided against.

Other major concerns with creating such a transition between a parallel plate transmission line and a coaxial cable have been noted in the past. Parallel plates operate with fringing fields that cause the electric field to not exist as a TEM field, like a coaxial, or a TE mode field like in a waveguide [22]. This more complex field geometry can cause return losses. It is often decided to regard the parallel plate field as a quasi-TEM line for purposes of calculating the geometry of these transformers [23].

CHAPTER 2

METHODS

This chapter details the various methodologies used to design, fabricate and test the geometric transformer. Each version of the transformer was first simulated to determine expected performance of the transformer iteration. The transformer was then fabricated in the machine shop provided by UMKC. Experimental testing was performed on the transformer in isolation as a comparison to simulated results and was performed in tandem with other components of the array.

2.1 Simulation Tools

The primary methodology through which the transformer was designed was with the use of full wave EM solvers. EM solvers are specialized software that are equipped to solve Maxwell's equations when given specific parameters and describe how an EM field will work under those parameters. They are commonly used in the making of transmission lines, integrated circuits, circuit boards, etc. The solvers I use are described as "full wave" because they employ all of Maxwell's equations in solving as opposed to a subset.

With the increase of complexity that modern electronics contain, including exponentially more individual instances of inductance, capacitance, resistance, etc., full wave EM solvers need to employ simplified methods to accurately solve

the field equations in an acceptable amount of time. Two methodologies are common in EM solvers: finite element method (FEM) [24] and finite difference method (FDM) [25]. These methods both portion the model into parts and use linear algebra to transform it into a sparse matrix. With that, mathematical tricks such as sparse factorization can be used to simplify the model without a loss of accuracy.

The full wave EM solvers utilized in this paper are CADFEKO software [26] and COMSOL software [27]. CADFEKO is a part of FEKO software developed by Altair Engineering. The software is designed as a general-purpose electric field equation solver and uses finite element method. This software was utilized in this project primarily in technical design.

COMSOL is a Multiphysics simulation software and also uses the finite element method for electric field simulations. COMSOL is equipped with a more robust time-domain simulation application. COMSOL can also simulate with pulses that we derive from the pulse forming transmission line. For these reasons, COMSOL was utilized primarily in simulating manufactured designs of the transformer.

The arbitrary transmission line calculator (atlc2) was also used in the design process [28]. Atlc2 is a windows program that utilizes Maxwell's equations as well as faraday's law to quickly provide precise impedance, capacitance and inductance of cross sections of a component. Accurate impedance measurement

is especially useful as the efficacy of the transformer is tied to the change in impedance across its length. While CADFEKO was used for the design process, atlc2 was used in conjunction to fine tune the transformer.

Fusion 360 was used for 3D modeling necessary in the production and fabrication of the transformer, which is a modeling software that is a part of Autodesk [29]. A full 3D model is used directly in 3D printing and is necessary in hand crafting as a guideline tool.

2.2 Test Methods

While simulation work was performed in the design process of the transformer, each iteration of the transformer was tested experimentally through several methods to determine the electrical properties of the transformer and how well it performs its task.

The first experimental method of testing the transformer is with a vector network analyzer to obtain scattering parameters [30], as well as impedance through time domain reflectometry [31]. A vector network analyzer is a device designed to measure scattering parameters, by using two ports and sending a test frequency through the device, while measuring power reflected and transmitted. Before use, the vector network analyzer must be calibrated by using a series of open loads, resistive loads, and shorted loads so that the vector network analyzer

can learn the scattering parameters of the cabling used to attach to the transformer, thereby allowing the device to filter out the effects of the cabling on the overall scattering parameters. The vector network analyzer can then give true scattering parameters of the transformer.

Additionally, the vector network analyzer has the ability to perform time domain reflectometry measurements. Time domain reflectometry operates similar principles as radar. Time domain reflectometry works by sending out a waveform across a conductor and listening to any reflections of the waveform. Waveform reflections are caused by discontinuities in impedance, which means that if the impedance is of uniform impedance and is properly terminated, then there will be no reflections. If a reflection is detected, then the device can use how long it took for the reflection to return to determine where the impedance discontinuity is.

An issue arose when the transformer was tested for scattering parameters. The method for testing scattering parameters with a vector network analyzer requires both ends of the transformer to be connected to two ports. However, only the coaxial line termination can be connected to the vector network analyzer. To properly connect the transformer to the vector network analyzer, we needed to fabricate two separate transformers, and connect the parallel plate ends to each other, creating a transformer that transitions from a coaxial cable into a parallel plate and back into a coaxial cable. The two coaxial ends can now be

attached to the vector network analyzer and the scattering parameters can be tested. However, as the testing frequency is transmitted through two transformers, the scattering parameters of the two transformers will be different than that of just one, specifically they will be roughly twice as lossy. The scattering parameters obtained from the vector network analyzer therefore needs to be adjusted to approximate what the scattering parameters would be for a single transformer.

Performing this adjustment is a relatively simple calculus. The loss of each transformer is compounded multiplicatively. For example, if each transformer has 90% power transmission, then the two transformers in sequence will show 81% power transmission. As the gain given by the vector network analyzer is represented in decibels, this means that the gain is halved. While a simple calculation, this is still an approximation as the performance of the two transformers are not necessarily equal. Therefore, the scattering parameters obtained by the vector network analyzer should be taken as scaled average performance of two separate transformers.

Along with the vector network analyzer testing, the transformers were also testing in practice with the bipolar pulse forming transmission line. The BPFTL is specifically constructed to be compatible with the transformer being tested. These in-practice tests are done with the laser emitter and the output is run through an attenuator and measured with an oscilloscope. The BPFTL is usually charged up to

a maximum of 500 V for these tests, as using a higher voltage on the oscilloscope requires a more robust attenuator that is impractical to set up for early testing.

The transformer is also experimentally tested with a power radiation probe. The device is used by exciting the transformer with the vector network analyzer and using a probe to act as an antenna and measure the power radiated from the transformer for any given distance and angle. These measurements are used to determine the efficacy of different shielding techniques.

2.3 Fabrication Methods

Multiple dielectric materials were used in the manufacturing of prototypes that were experimentally tested (see table 1). The most important aspect of the material to take into consideration was its dielectric constant, which impacts the impedance of the transformer, and affects the speed at which a pulse transmits through the transformer. The speed of the pulse is important as the transmission of a pulse, and any reflections, are connected to discontinuities of impedance within the transformer. If the impedance changes rapidly then the reflection is more severe than in the impedance were to change the same amount but more gradually. While a higher dielectric constant may seem to slow down a pulse by an imperceptible amount, for example reducing the speed from C to .75C, this

Material	*Dielectric Constant*	*Dielectric Strength*	*Temperature Maximum*
Rexolite	2.53	50-kv/mil	176 C
ABS	2.9	12-kv/mil	110 C
Resin	3.11	20-kv/mil	130 C
ro3010	10.2	35-kv/mil	150 C
Foam PE	2.3	25-kv/mil	200 C

Table 1. Dielectric materials used for this transformer

change will significantly change how gradual the pulse sees the impedance shift and will lower reflection [32].

Changing the dielectric constant can also create a change in the pulse shape, even with less reflections. If the pulse is transmitted over materials with differing dielectric constants, the frequencies within the pulse are stretched or compressed, similar to the doppler effect. In our cases, preserving the pulse shape is just as important as mitigating reflections and losses, so a material was chosen with both qualities in mind.

The dielectric material also needed to conform to a standard of accessibility, affordability and practicality. Many of the dielectric materials used for the transformer were substances that could be manufactured in a 3D printer such as SLA resin, which has a dielectric constant of 3.5. 3D printers are devices

that when given a 3D CAD model, can recreate the model using quickly hardening polymers. 3D printable materials were a very attractive choice as there was no shipment of material necessary in most cases, the shape of the device could be designed solely in software, and hand cutting the dielectric material was unnecessary. These qualities allowed for very quick turnaround in the fabrication process.

However, these materials have their own set of drawbacks. Most prominently, by the nature of 3D printed material, these dielectric materials have a relatively low melting point. A material with a low melting point makes it difficult to properly solder wiring on or around these dielectric materials without risking material deformation. Additionally, under high heat the material could undergo carbonization [33], which could potentially change the dielectric strength of the material, making dielectric breakdown more likely [34, 35]. Additionally, 3D printers have a natural size constraint, and the 3D printer used in the university's machine shop could not print anything with a dimension higher than 12 inches. If a larger object were needed to be printed, it would need to be printed in pieces and connected afterward, which has the potential to leave impedance discontinuities and points of probable dielectric breakdown [36].

An alternate option to 3D printed dielectric was simply ordering a specific material and cutting it by hand. Hand fabrication carries the benefit that far more flexibility is allowed in the choosing of a material with a specific dielectric

constant, as well as other important properties such as its melting point and coefficient of thermal expansion. The material is also not restricted to any reasonable size so long as the material is ordered in a large enough segment. The major drawback to hand fabrication would be higher difficulty in manufacturing exotic shapes, which 3D printing excels at. Rectangular shapes and tapered pieces are doable, but shapes such as cones are too impractical to cut by hand. Additionally, ordering and cutting material is more expensive and time consuming.

Many prototype designs used multiple dielectric materials and were able to combine the strengths of each. Early prototypes utilized a hand cut taper made from Rexolite, which is a material with an optimal dielectric constant and a very high dielectric strength. These designs also used a conic shape that was 3d printed and epoxied to the Rexolite. The cone was thin enough that the minor difference in dielectric constant between the materials would not create a significant change in impedance or wave pulse transmission speed.

The transformer needs a conducting material to transmit the energy across and to shape and contain the EM field to prevent issues such as mutual coupling and radiated energy. The material needs a high conductivity, which is the quantification of how well that material conducts current without losses to resistance and heat [37]. Additionally, when transmitting frequencies through a parallel plate or waveguide, the conducting material's skin depth must be taken into consideration. The skin depth measures how far an alternating current of

some specified frequency penetrates the conducting material [38]. Higher frequencies will penetrate less, and some conducting materials are better suited for lowering skin depth. If the skin depth significantly exceeds the thickness of the conducting material, the efficacy of the material as a conductor and as shielding from EM radiation will be reduced [39].

Choosing a conducting material is a simpler choice when compared to the options for the dielectric material. At the bandwidth of frequencies that the transformer is designed to operate at, around 600-Mhz to 1500-Mhz, the skin depth of most conducting metals that are practical for use in the transformer will not exceed 5-µm, in most cases being significantly smaller. Any conducting strip that is 1 mil or thicker will have no problems with skin depth in this transformer. Most conducting materials will operate sufficiently for this transformer.

Other considerations in choosing a conducting material is conductivity, affordability, and practicality. Choosing a material with a particularly high conductivity can mitigate resistive losses, although the value of mitigating these losses should be weighed against the price of the material and how much impact these losses have on the overall performance of the transformer. A material such as copper has a relatively high conductivity while also being affordable when used for small strips, and easy to cut and manipulate, making it very practical for quick and precise fabrications.

A common method for implementing the conducting material is with hand

cut strips attached with adhesive. Using copper foil approximately 2-mil thick, it can be cut with an X-acto knife and a paper template to any shape needed for the conductor of the transformer. The copper foil then has a thin layer of adhesive applied to it with an adhesive sheet and can be affixed to the dielectric. Copper strip attachment is the quickest and easiest method of attaching the conducting material. Copper strip attachment does have some drawbacks, most notably the lack of precision inherent to hand crafting the material. The active plane on the transformer is the most sensitive part of the transformer, and a slight misplacement or miscut could change the impedance of a portion enough to impact transmission. For prototypes and proof of concepts copper strip attachment is a sufficient method of applying the conductor, but it will inhibit optimization.

The alternative method of applying the conducting material is with one of the several machine application methods. Copper etching is a method that is commonly used for PCB creation [40]. It works by plating a PCB with copper and a strong acid is used to remove the copper from the PCB. Portions of the copper is protected from the acid by a “masking” material, that allows the etching to give highly complex copper designs on the PCB. While copper etching is most commonly used for PCB making, it can also be used for other purposes, such as in making geometric transformer, so long as the design of the transformer conforms to a similar shape of a PCB board.

Electroplating is another method to apply a conductive material, through the reduction of cations in a metal induced by an electric current, which then flow through an electrode onto the surface of the dielectric component that is to be coated [41]. Both copper etching and electroplating are time consuming and are generally used for precision work on a final product.

The conducting material is generally connected via soldering. Soldering is a method of using an alloy that melts at low temperature, such as tin, to connect conducting materials together by applying the alloy to the materials with a heating implement, and allowing it to cool and harden with the components connected. In situations in which heating is dangerous to the integrity of the component, it may be appropriate to connect the conductors together mechanically, in which the conductors are simply pressed together by mechanical tools such as nuts and bolts.

CHAPTER 3
TRANSFORMER

3.1 First Design

The production of the transformer began with the approach to smoothly introduce the parallel plate geometry to the coaxial geometry. Before we looked deeply into mutual coupling, fringing fields and radiation, we focused on ensuring a design that would connect the two differing geometries that avoids unnecessary creases or corners. The reason for this was simple, we knew that the transformer could not operate without the transformers in proper contact with one another, and we reasoned that hanging conductors and unnecessary corners could present their own problems in the future. We knew that the parallel plate input was of a 50-Ω impedance, and we knew that the coaxial output was also of a 50-Ω impedance. As long as we ensured the geometry matched with the parallel plate and coaxial elements, and used dielectric material of the same dielectric constant, then the transformer would at least smoothly connect with the two elements themselves, and we would simply have to ensure proper transmission within the transformer, isolating the problem to the task at hand.

Approaching the design from the perspective of upholding continuity led to the basic design geometry of a tapered dielectric and a half-cone (figure 7).

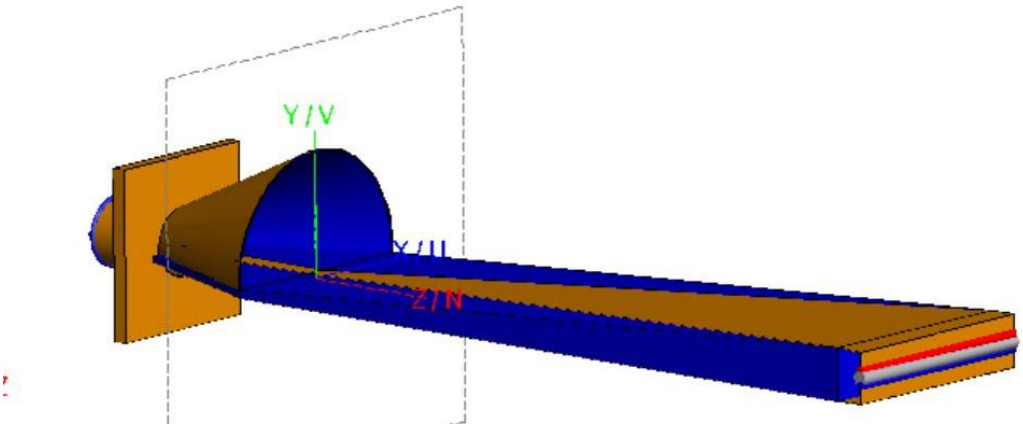

Figure 7. Original cone and taper design. The active plane tapers inward while the ground plane stays flat and wraps around the cone. This design also included a build in plate for connection with the coaxial cable; this feature was removed as it was determined to be easier to connect the LMR 600 cable directly to the cone.

With the taper design, the geometry begins identically to the parallel plate element. The active plane and ground plane are of equal widths and use the same dielectric.

Along the length of the transformer, the active plane shrinks and slants inward toward the inner conductor of the coaxial. It was necessary to taper the active plane because there was a larger gap between the active plane and the ground for the parallel plate element, compared to the coaxial. We wanted the ground to be flat on the bottom, for simplicity when testing, so the active plane had to taper downward to bridge that gap. This taper design was partially based on similar designs of tapered transmission lines and tapered impedance transformers. These

transmission lines are made based on the knowledge that the simplest way to change impedance in a parallel plate transmission line is to change either its width or thickness, giving control of the impedance to the designer [42]. For our purposes, we would use the same equations but adjust the width and thickness to ensure that the impedance remains static. Nearing the coaxial element, the ground plane would wrap around the active plane until it reached a full surround of the active plane, similar to a coaxial design. The end of the transformer would further shrink until it possessed equal dimensions to an LMR 600 type coaxial cable

Part Description				
Part Number	Application	Jacket	Color	Stock Code
LMR-600-75	Indoor/Outdoor	PE	Black	54148
LMR-600-75-DB	Outdoor	PE	Black	54220

Construction Specifications			
Description	Material	In.	(mm)
Inner Conductor	Solid BCCAl	0.108	(2.74)
Dielectric	Foam PE	0.455	(11.56)
Outer Conductor	Aluminum Tape	0.461	(11.71)
Overall Braid	Tinned Copper	0.490	(12.45)
Jacket	Black PE	0.590	(14.99)

Figure 8. Specifications for LMR 600 coaxial cabling

(figure 8). We did not initially attempt to build the transformer to connect with the coaxial port that connects to the antenna element, as that was also still under design. The LMR 600 cable was a close approximation to what the coaxial port would become, and we knew any differences could be adjusted for.

The taper and cone design was additionally beneficial for being simple to simulate, construct and test. These initial simulations were performed through CADFEKO software and focused primarily on testing how minor changes to the transformer's geometry would impact scattering parameters and the transformer's reflection coefficient. Initial simulations of the taper and cone design revealed low transmission, generally below 20% power transmitted, with most of the lost power being reflected backwards. Further changes to the degree that the dielectric is tapered, the degree that the active plane is tapered, and the size of the cone revealed a significantly better transmission, around 80-90% for varying designs across an ultra-wide bandwidth (figure 9, figure 10). The key to these results were not necessarily in achieving optimal power transmission, but in achieving satisfactory and even power transmission across an ultra-wide bandwidth from 600-Mhz to 1500-Mhz.

After this first round of simulations, we were able to take our most optimized design and work toward fabrication, so we could have a baseline for comparison between how the tapered balun transformer performs in simulation

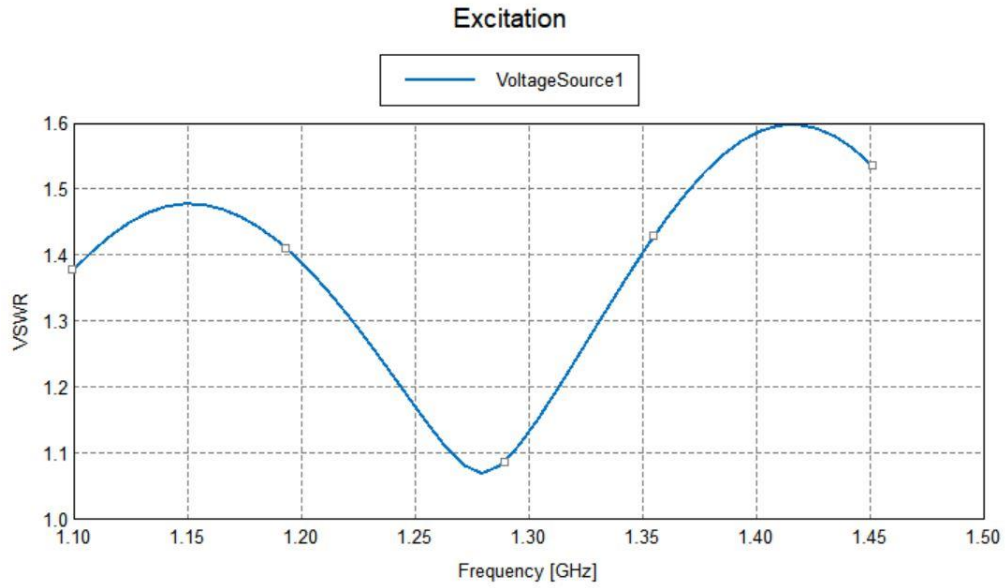

Figure 9. Voltage standard wave ratio of the first cone and taper transformer design simulated in CADFEKO.

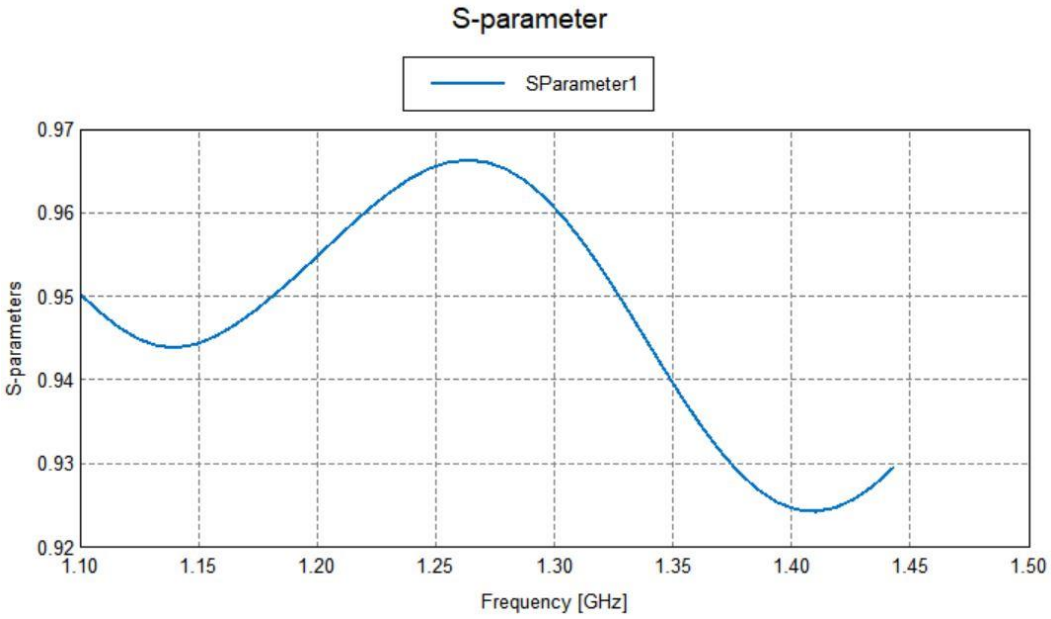

Figure 10. S21 scattering parameter of the first cone and taper transformer design simulated in CADFEKO.

and how it performs experimentally. The first step would be the decision on what materials would be used in the fabrication, and how it would be fabricated. The material chosen for the tapered dielectric was decided to be Rexolite, for having a high dielectric and thermal strength, while having a dielectric constant equal to the material used in the parallel plate element. The Rexolite would have to be ordered offline and would be cut using the machinery in the university's machine shop. Testing showed that the material of the cone would be sufficient as long as its dielectric constant was within a <.5 range of the Rexolite. The cone was thin enough that a small disparity of dielectric constants would not significantly impact performance. The material chosen was ABS, a cheaper material that could be manufactured in the university's 3D printer, which was important as it would be a difficult and time-consuming task to make a cone like that by hand.

The dielectric material was then taken from the 3D models in CADFEKO and made into item request specification sheets proper for the fabrication of the transformer.

2-mil sheets of copper were used as the conducting material. This conducting material was first placed onto the Rexolite dielectric material, using adhesive strips, and was then cut into the taper shape. The cone was attached using epoxy resin, and the outside ground conducting material was first cut and

then wrapped around the cone to create a full surround of the active plane. Finally, a piece of LMR 600 coaxial cable was cut and stripped of its insulation, at which point the inner conductor was soldered onto the active plane and the outer conductor was soldered evenly across the cone and base of the transformer. This

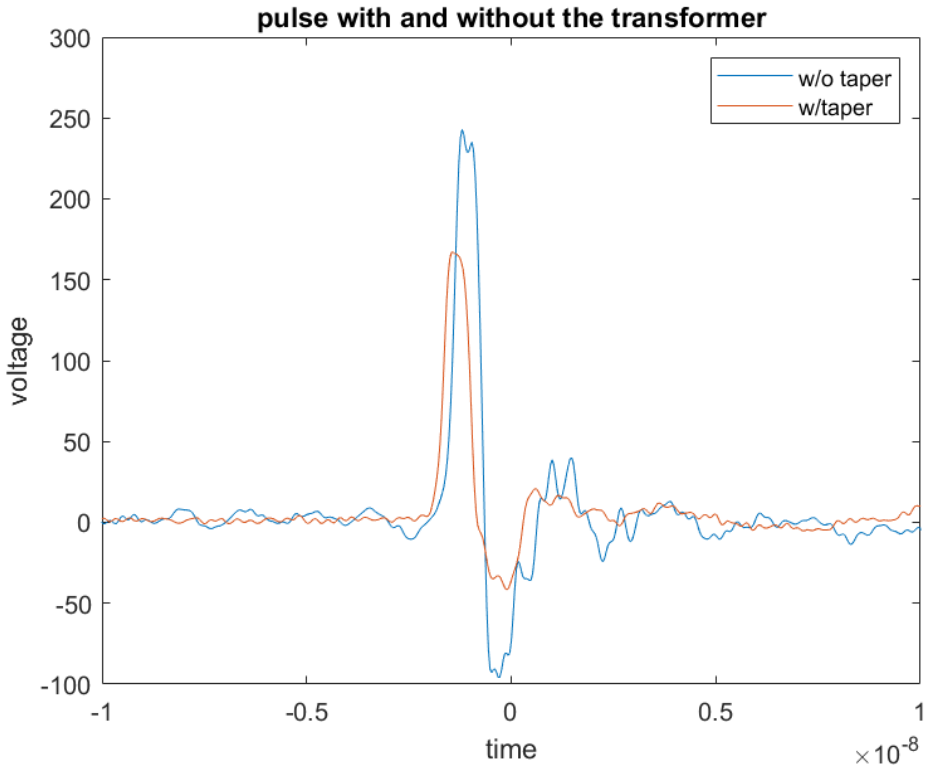

Figure 11. Pulse generated by the pulse forming transmission line, before and after it passes through the first cone and taper transformer design. A probe was used to determine the pulse shape directly out of the pulse forming transmission line, while the pulse out of the transformer was inserted into an oscilloscope via coaxial. Because of this, the pulse measured by probe is not precisely accurate to pulse generated by the pulse forming transmission line, but it does accurately present peak voltage and power transmitted. With this, we can determine that the transformer reduces peak voltage to approximately 70%.

process was performed twice to obtain the necessary two transformers.

Experimentally testing the transformer was successful in that it showed promising results, with tests in tandem with the pulse forming transmission line showing similar results to testing. Initial tests with the pulse forming transmission line with a probe showed minimal distortion to the shape of the pulse, although it was noticeably attenuated (figure 11). Testing with the vector network analyzer also gave results similar to simulation in the scattering parameters across the bandwidth of the transformer (figure 12, figure 13). When we performed time domain reflectometry, we saw noticeable points of discontinuity in the impedance across the transformer, on the space where the half-cone began, as well as in the connection to the LMR 600 coaxial cable. We were able to use this information to begin the design of a second model that would hopefully eliminate these problems and give superior results.

To properly ensure that the impedance across the length of the transformer was consistently 50-Ω, an arbitrary transmission line calculator was used to determine the impedance of the transformer at cross sections at given intervals. The arbitrary transmission line calculator can determine the impedance, as well as other electrical properties, of the cross section of the transformer by using a bitmap that is color coded to represent the positive plane, ground plane, and specific dielectric materials. Using the arbitrary transmission line calculator, we found that there was indeed a high amount of impedance in the areas that the

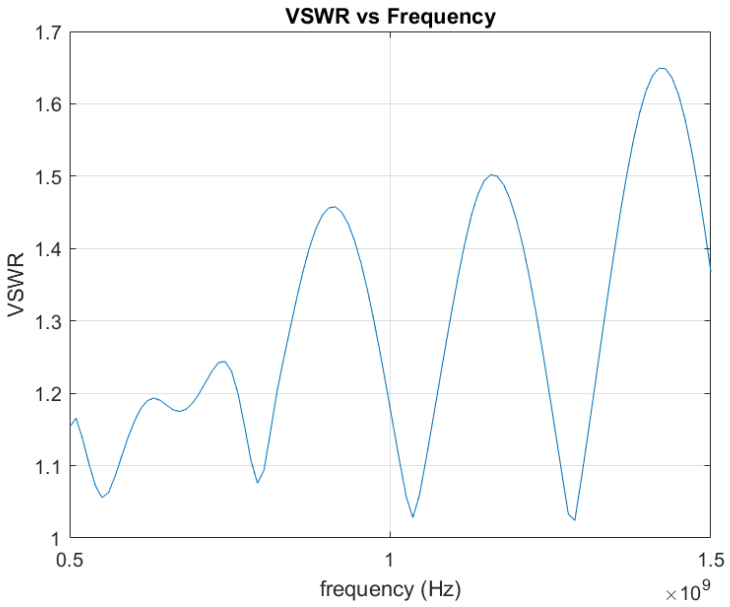

Figure 12. Voltage standing wave ratio of the first cone and taper transformer design, measured experimentally with the vector network analyzer. The vector network analyzer requires two transformers, set end to end to properly measure the properties of the transformer. This figure adjusts the VSWR to account for this and present the VSWR of one transformer.

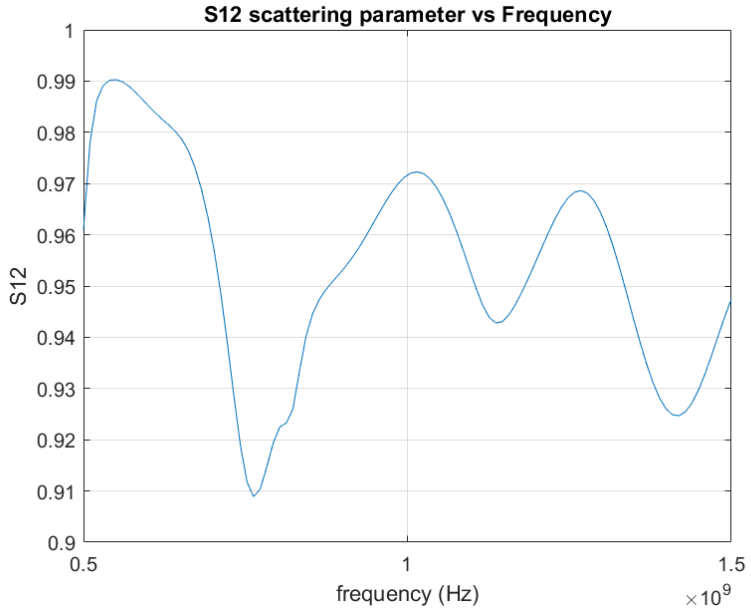

Figure 13. S12 scattering parameter of the first cone and taper transformer design. this figure is adjusted for the same reason as the VSWR measurement.

time domain reflectometry test claimed.

3.2 Second Design

To mitigate the aforementioned concerns, a change to the half-cone was introduced, by slicing it downward into a crescent, so that there would not be an abrupt change in impedance caused by the ground plane wrapping around the active plane (figure 14). Additionally, a groove was introduced to the end of the transformer meant to connect with the coaxial element; this design element allows for a more secure solder connection with the coaxial line. Other minor changes were added as well, such as shortening the length of the transformer and slightly changing the shape of the active plane, to further facilitate an even impedance across the length of the transformer. In simulation, this transformer demonstrated improved transmission across the 600-Mhz to 1500-Mhz bandwidth.

Construction of the taper and crescent cone version of the transformer was like the first, with one key difference being that an external brace was added to the coaxial connection, to stop the soldered coax connection from shifting around (figure 15). It was found that this shifting could cause significant changes to the impedance in the area that the coaxial element is soldered to and was likely contributing to the earlier impedance discontinuities seen earlier.

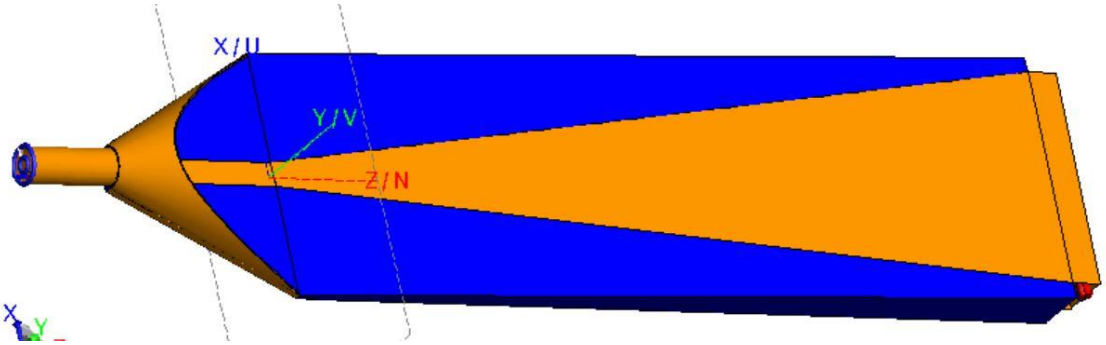

Figure 14. Model of the second cone and taper design. this design cuts the cone into a crescent shape to mitigate impedance discontinuities.

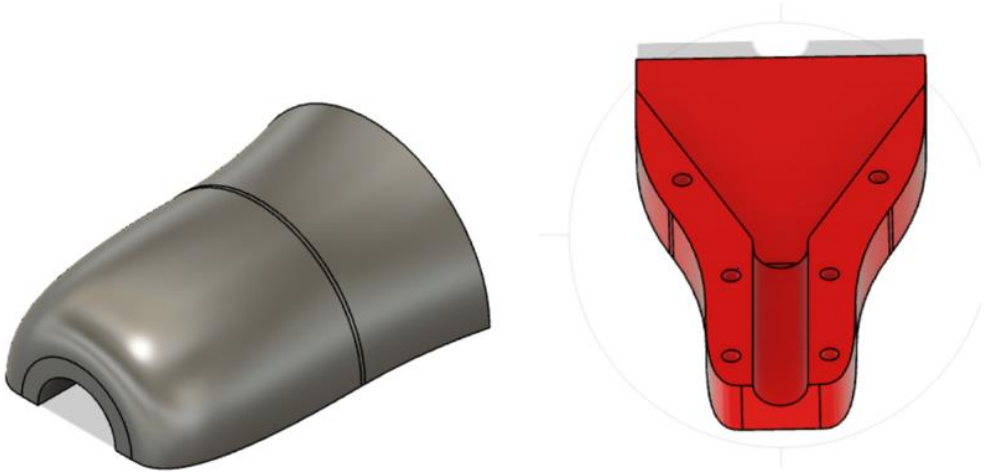

Figure 15. Brace built from ABS to support the connection between the transformer and the coaxial. The cone section rests within the casing and the two pieces are screwed together.

As this improved version of the transformer was tested, we saw likewise an improvement in transmission across the bandwidth, as we had seen earlier (figure 16, figure 17). Time domain reflectometry confirmed that we had significantly reduced the impedance discontinuities, although some less significant (<3-Ω) discontinuities remained. When pulse testing with the pulse forming transmission line, we saw an improvement over the original design, with only minor attenuation

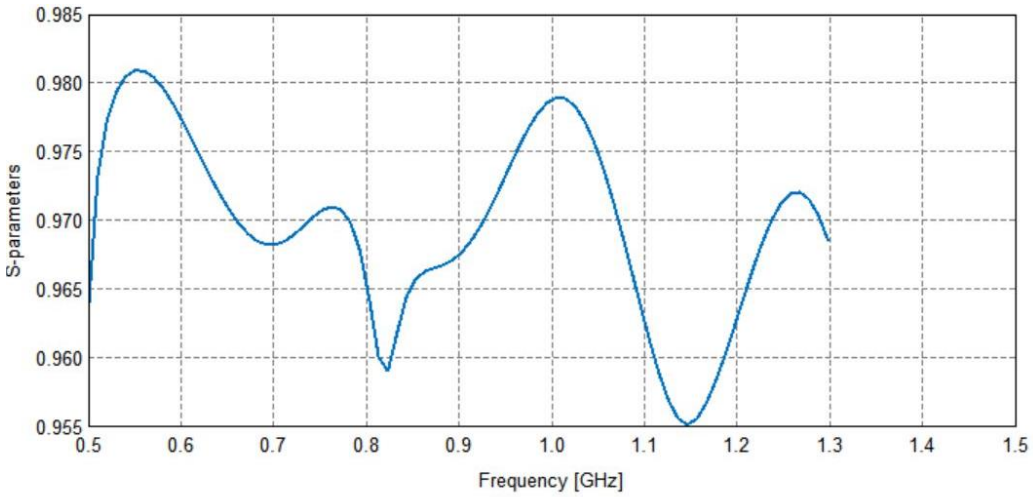

Figure 16. S21 scattering parameters of the second transformer design, simulated in CADFEKO software.

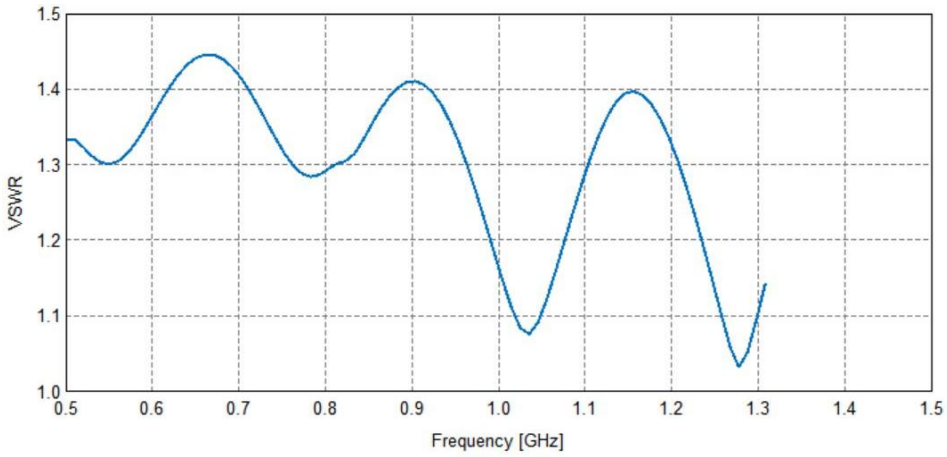

Figure 17. Voltage standard wave ratio of the second transformer design, simulated in CADFEKO software.

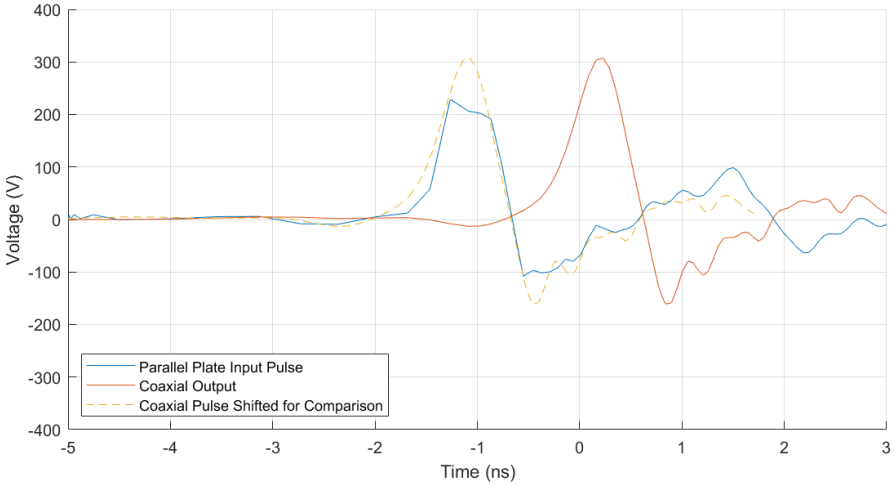

Figure 18. Experimental pulse comparison. Probe testing cut off the top of the pulse, though we can see the pulse shape is preserved. Simulation testing approximates peak voltage is reduced to around 90%.

of the pulse and the pulse shape and length being maintained well (figure 18).

A problem arose when we began high-power pulse testing with the pulse forming transmission line. We had not done pulse testing over 200 V before, but in these tests, we began testing at higher voltages to see if the transformer operates differently under higher power, or to see if any coronas or electrical breakdown might appear. As we raised the voltage to around 600 V however, we began to see some of the equipment in the room begin to act negatively to the tests. We immediately shut down testing to avoid damaging anything and theorized that the transformer may be radiating more energy than we had anticipated.

We began a radiated energy probe test and saw that we were correct in our theory. The probe confirmed that about 10% of energy losses were from the energy radiating from the transformer. Radiated energy was of course a concern in energy loss, but the larger issue is that it became clear that the transformer would not operate properly as a part of an array like with excessive power radiation.

The first step we took was in building a temporary enclosure for the transformer so that high power testing could continue. This enclosure was also necessary as the transformer was necessary for testing the pulse forming transmission line without a probe.

Using a far field gain tool within CADFEKO, we were able to simulate the

transformer and compare how power is radiated when it is alone and when it is inside our temporary shield to verify that the temporary shielding is satisfactory (figure 19, figure 20), and to have a starting point for building a new transformer design that is self-shielded.

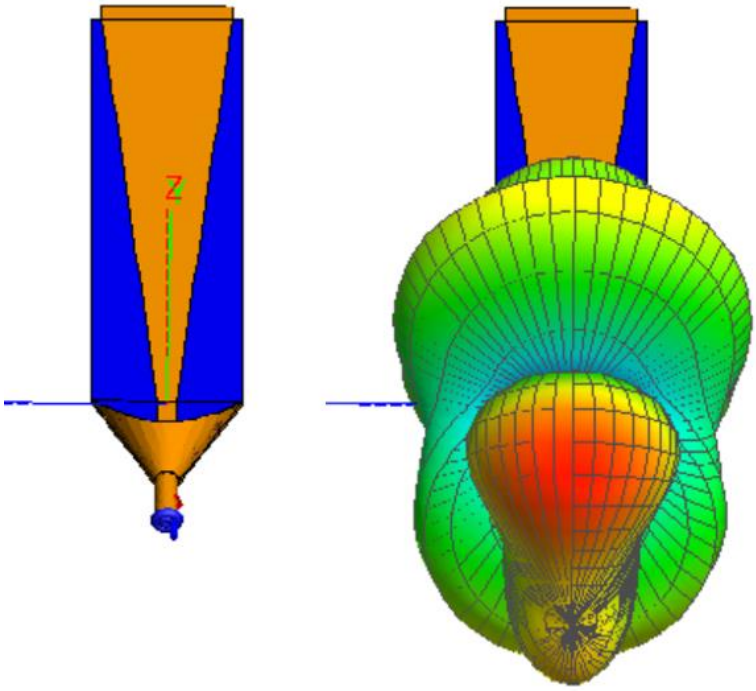

Figure 19. Radiated energy simulation though CADFEKO. Peak gain is .08 outwards from the coaxial element.

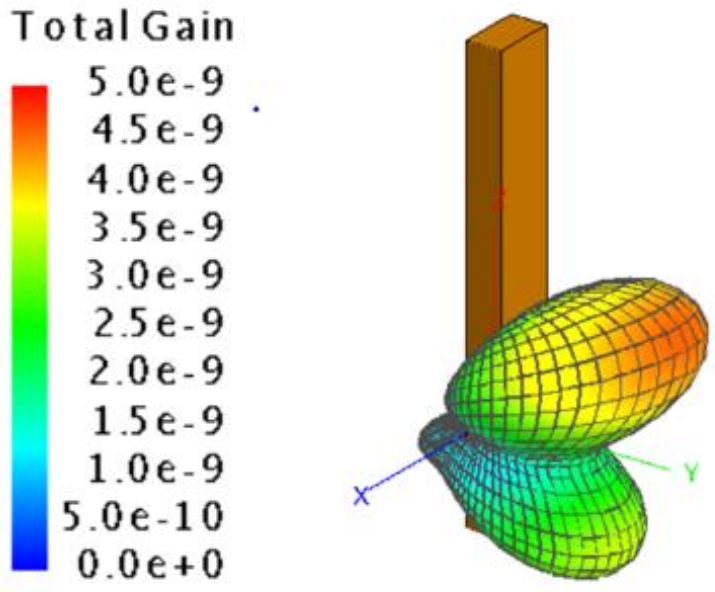

Figure 20. Radiated energy simulation of the transformer through shielding. Peak gain is 5.0 e-9.

3.3 Third Design

As we engaged a new design, we also took into consideration the elimination of concerns such as electric breakdown and mutual coupling. Using CADFEKO, we were able to construct a current density field graph, that demonstrates where the current density is highest in our current design (figure 21). Current density reaches peaks around corners in the active plane, so we knew that to eliminate the potential for electric breakdown, we needed to make the geometry of the transformer more uniform [43]. Additionally, concerns were raised about the

current temporary shielding, that the additional conducting material could inadvertently create an additional transmission line and facilitate increased reflections. To shield this new design, we knew that we must use the main ground plane to fully shield the transformer, which would be simpler to design and construct, reduce the potential of breakdown between conductors, and eliminate reflections created by the enclosure, as well as reduce losses from radiated energy and avoid mutual coupling between neighboring elements in the array.

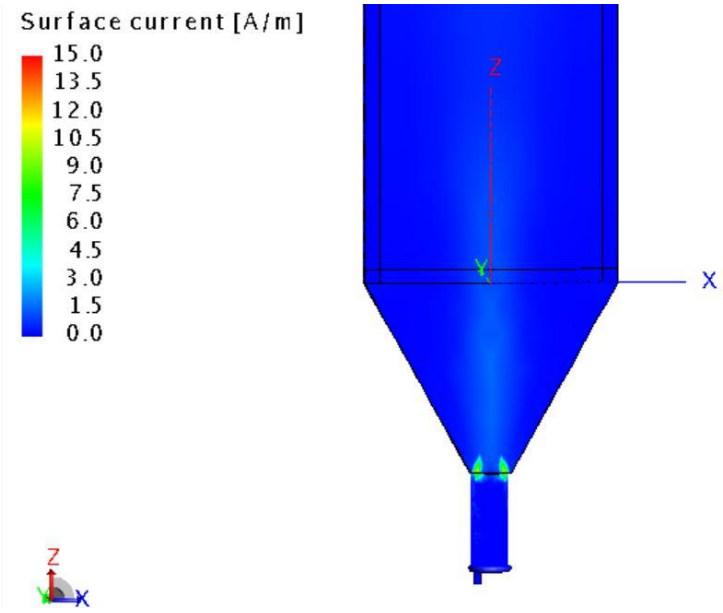

Figure 21. Surface current density graph simulated in CADFEKO. Current density is normally spread out very evenly, leaving little danger of electric breakdown. However, corners in the wrong spot can create point of high current density, seen in green here.

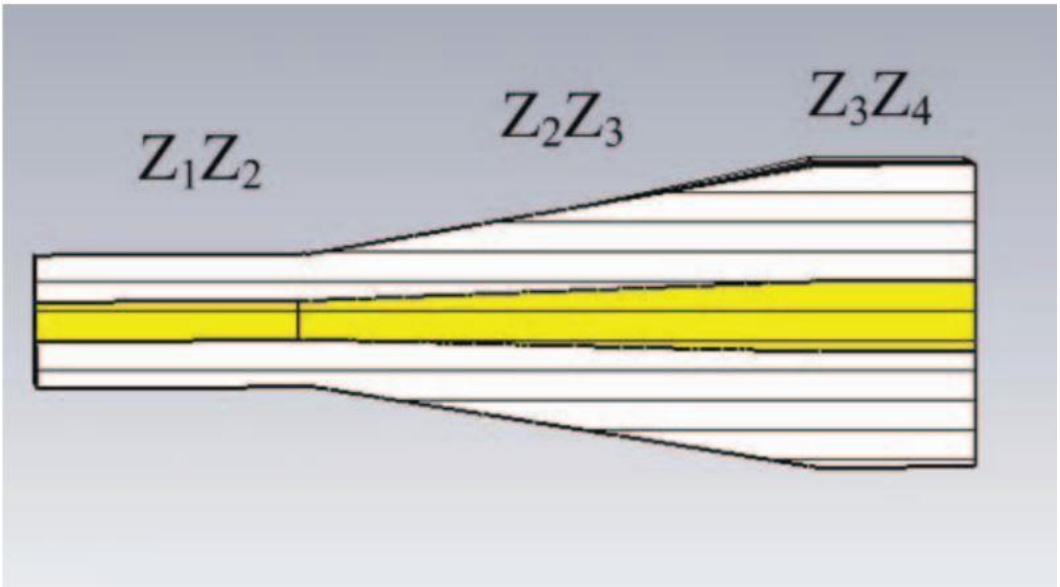

Figure 22. Model of GTEM transition line from Design of Ultra-Wide band transition Connector for GTEM Cell. This model was used for our third design because of its similarities with the first two designs.

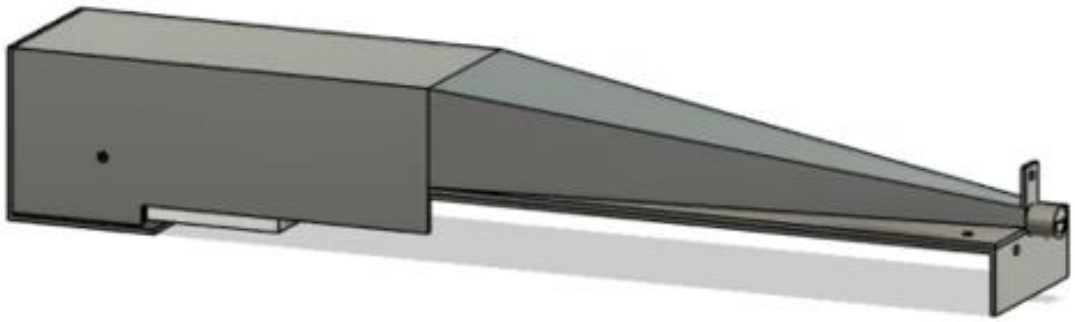

Figure 23. Model of the third transformer design, based on the principles of a GTEM cell. the shielding additionally encloses the pulse forming transmission line for optimal reduction of radiated power.

We decided to modify the taper and cone design into a design derived from TEM (transverse electromagnetic) cells. TEM cells are already made to contain radiation, as well as being less prone to breakdown. Keeping the taper on the active plane, the ground plane now encloses the transformer and parts of the pulse forming transmission line. We were able to streamline the taper and conducting material to eliminate corners on the active plane.

TEM cell designs are ideal for our purposes because they cover our requirements while being simple enough to modify and optimize. Many TEM cell designs are fed via a coaxial cable, operate at high power, and can be designed to emit minimal radiated power. The functionality of a TEM cell operates similarly to a parallel plate that is being excited by a coaxial line. TEM cells are also reciprocal networks, so there is no inherent problem with using the design to have the coaxial line being excited by the parallel plate.

The new transformer design borrows from the GTEM cell transition found in *Design of Ultra Wide band transition Connector for GTEM Cell* [44] (figure 22). This design was chosen because it is ultra-wideband, designed to operate at high power, and is excited by a coaxial line. Additionally, the GTEM cell transition already uses a similar tapered dielectric design that we had been working with in our previous iterations of the transformer.

However, much of the design of the GTEM cell transition had to be modified. The primary change is that the GTEM cell transition uses a “concentric

square design" to simplify much of the calculation necessary to ensure even impedance across the width of the transformer. However, to properly connect with the pulse forming transmission line, we could not maintain the concentric square design. To calculate the appropriate dimensions to keep the transformer at 50 ohms at the forepart, we used an arbitrary transmission line calculator (atlc2). The arbitrary transmission line calculator allowed us to implement a cross sectional design that is symmetrical in only one dimension. The same can be done with the rear part section connected to the coaxial (figure 23).

Building the full transformer is a matter of smoothly transitioning between the coaxial and parallel plate ends. Additionally, we were able to use dimensions given to us for the coaxial connection for the antenna array, instead of using the LMR 600 stand in coaxial element.

The enclosed design would enclose portions of the pulse forming transmission line as well, which came with some benefits and drawbacks. The purpose of doing so was to ensure full electromagnetic enclosure, which will minimize radiated power, which is necessary for the transformer to act as a part of an array, as well to mitigate some radiated power losses [45]. Additionally, sharing the ground plane allows any reflected power to be diverted through the pulse forming transmission line's heat sink, eliminating the potential for reflected power to damage other components in the system. However, enclosing portions of the pulse forming transmission line changes the impedance of the line, and the

shape of the line had to be changed to correct the impedance, as well as the shape of the parallel plate element that the transformer connects with.

In simulation, the new enclosed design performed significantly better, exhibiting a very high-power transmission (>99%) over the 600-Mhz to 1500-Mhz frequency band (figure 24). Through testing in COMSOL, we were able to simulate the transformer in time domain as the pulse taken from the pulse forming transmission line passes through it (figure 25). These simulations show a similarly

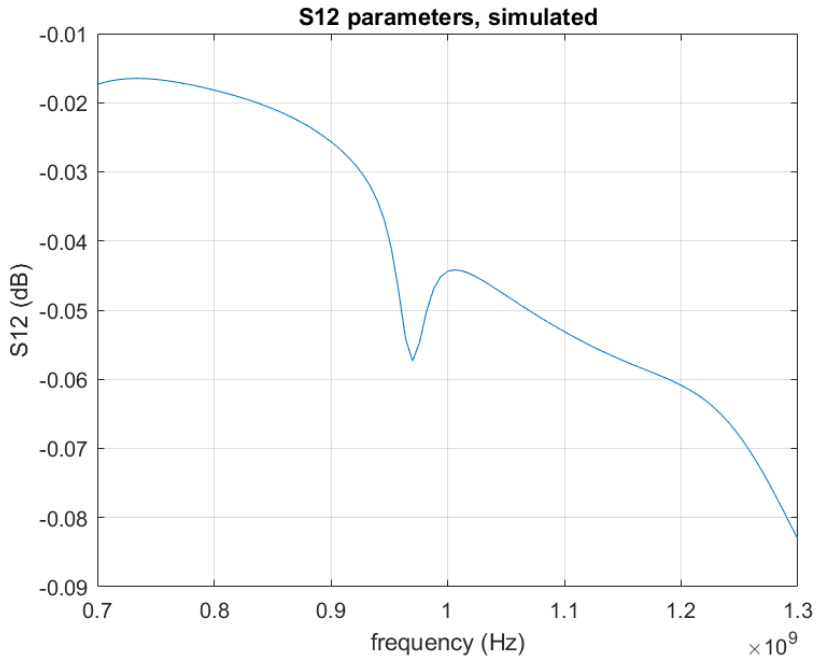

Figure 24. S21 Scattering parameters simulated through CADFEKO. This simulation shows >99% power transmission across the whole band.

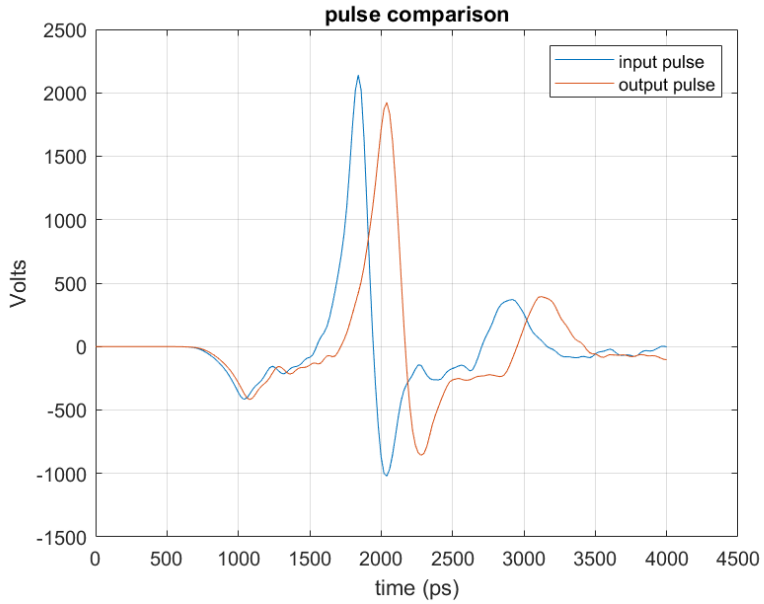

Figure 25. Comparison of pulse experimentally tested before and after transmission through third transformer design. Peak voltage is reduced to 95% with very little change in pulse shape.

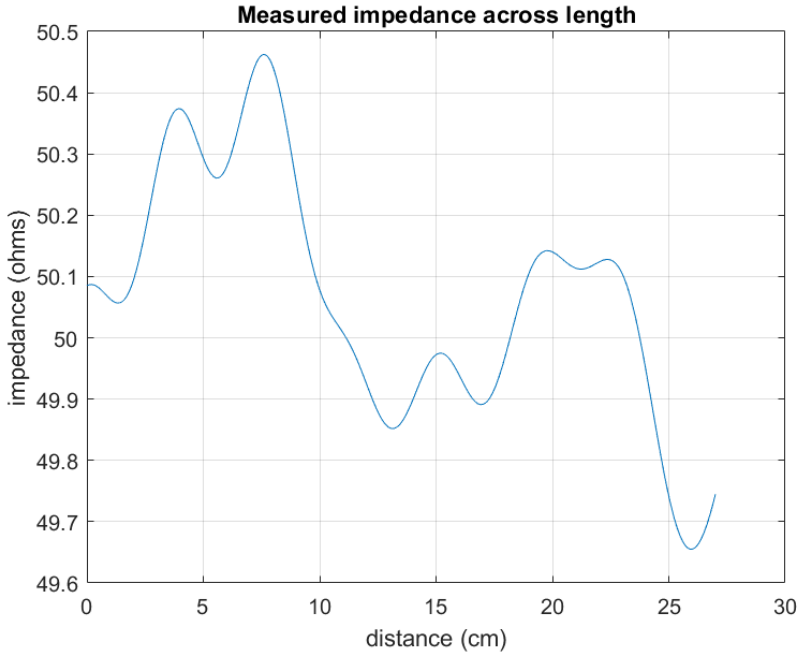

Figure 26. Time domain spectrometry of the third transformer design. Impedance discontinuity is very low, which reduces reflected power.

high-power transmission without significant changes to the shape of the pulse.

To fabricate the new transformer, we decided on an early 3D printed version and a more robust metallic version. The dielectric material used in both would be a 3D printed resin, the same resin used for the pulse forming transmission lines. The 3D printed resin eliminated the need for ordering out of house materials and cutting them with the shop. The dielectric resin has an adequate dielectric strength to ensure there is no danger of electric breakdown

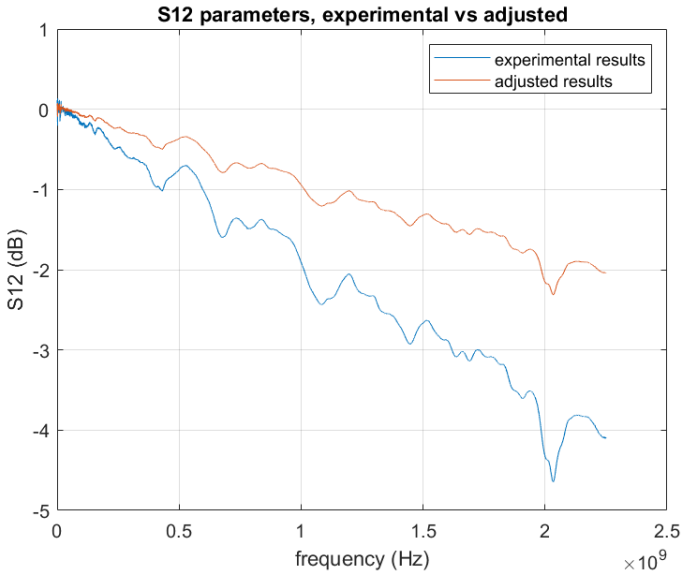

Figure 27. Final S21 scattering parameters for the third design. This figure demonstrates the difference between results given form the vector network analyzer, through end to end testing, and the adjusted results that give the value for a single transformer.

within the transformer at high power.

To form the enclosure for the 3D printed transformer prototype, a plastic casing is 3D printed and copper sheets would be fixed to the inside of the casing with adhesive. They are put on the inside of the casing so the plastic of the casing would not impact the impedance of the transformer. The ground plane of the transformer would be similarly 3D printed with copper sheeting fixed to it. The casing and the ground plane would surround the dielectric and are attached to each other with solder to create a full enclosure around the active plane on the dielectric.

A more robust prototype was also designed to create the enclosure with copper sheet metal parts, that don't need a 3D printed casing to hold its shape. The sheet metal would be bent and cut into shape and attached mechanically to each other with bolts. Mechanical connections would create a sturdier prototype, that is also more precise in its impedance across the length of the transformer.

In both transformers, the coaxial element connection would be attached mechanically with screws, as soldering pieces of coaxial to the active and ground plane gave too much variance in impedance at the connection.

In experimental testing, the new design of the transformer maintains an even 50- Ω impedance across the length of the transformer (figure 26). The transformer is shown to be similar in experimental results to how it was simulated. Most notably, the transformer contains good transmission across an ultra-wide

bandwidth, although slightly less transmission at higher frequencies (figure 27). The new enclosure allows for little radiated power. The enclosed version shows approximately 55 dB less radiated power when compared to the unenclosed prototype.

The new design of the transformer operates very well under the specifications given for the project. In cases where adequate power transmission is equally as important than maintaining the frequency content of the pulse across an ultra-wide bandwidth, the transformer is satisfactory.

Testing is still ongoing with the sheet metal design of the transformer. The new shielding will significantly mitigate the potential for mutual coupling affecting the performance of the transformer, although further testing is required.

CHAPTER 4
FURTHER PROJECTS

Continued work on balun transformer lead me to assisting in the construction of a project for a system, around the size of a suitcase, capable of using methodology similar to the pulse forming transmission line of the antenna array project (here called a blumlein), that functions as a square pulse generator. This project required the same type of geometric transformation, with a parallel plate input element and a coaxial cable output element, and the transformer is required to transmit high-power, high frequency pulses with minimal loss of power and minimal distortion of the pulse.

However, several key differences are present in this project that prohibited me from using the exact same design as in the antenna array project. The most notable difference is that the blumlein, contrary to the pulse forming transmission line of the array project, did not terminate at 50- Ω impedance, instead only terminating at 7- Ω. A smaller impedance on the parallel plate element is a major concern, as the output of the suitcase is still required to be a 50- Ω coaxial cable. As a primary source of reflected energy, and therefore energy loss, is from the discontinuity of impedance, the impedance change would inevitably lead to an amount of lost power.

Other changes include the shape of the pulse. Instead of the short sinusoidal pulse of the previous project, this project would be making a square

pulse, which requires a larger bandwidth to maintain its shape. Radiated power is less of a concern, as the transformer and blumlein would be isolated within a portion of the suitcase. Power lost or mutual coupling is still a concern, but less of a priority than in an array situation.

The major difference in how this transformer was to be approached was in the design of the impedance across the transformer. In the previous project, the goal was to simply maintain an even impedance across the length of the transformer, as mitigating impedance discontinuity is the best way to prevent reflected power. But with this project, the impedance must not be kept even, but instead carefully shaped across the length of the transformer to result in the impedance discontinuity that would result in the *least* reflected power and power losses.

This transformer needed to be considerably thinner as well, as the parallel plate element of the blumlein had a thickness of a mere 50 mil, or around 1.27 mm. It was decided that the transformer would not taper in thickness, and the coaxial element would not attach with the transformer as evenly as with the previous project. Alternate connection techniques with the coaxial element could be used that would lead to impedance discontinuities that were minor compared to the impedance discontinuity within the transformer. The reason for this choice was to allow the thin design of the transformer to be fabricated the same way as the blumlein, with copper etching on a strip of RO3010 dielectric material.

Fabricating a transformer with a thickness of only 50 mil would be difficult to do with 3D printing and even more difficult to fabricate by hand and would additionally be particularly fragile using 3D printed material.

Transformers that change impedance as well as geometry carry significant other facets that need to be taken into consideration. An impedance shift would necessarily lead to a voltage gain, which becomes more significant the larger the impedance shift. Each impedance transformer design can mathematically account for the impedance shift using the calculations of the electric field as the power is transmitted across the transformer, but the reason for the impedance shift is always the same. Following the fundamental principles of power transmission via electricity, we know that power can be described as voltage squared divided by the impedance. If the impedance is shifted up by a factor, the voltage must also shift up by the square root of that factor, if power is to be conserved. In the instance of a 7-Ω to 50- Ω shift, it is expected that the voltage shifts upward by a factor of 2.6, give or take when power losses are taken into consideration. The voltage shift needs to be considered when ensuring the transformer does not electrically break down, and high voltage shifts can cause corona effects around points of high current density in a transformer.

The design of this transformer is an exponential transmission line transformer. The reason an exponential transmission line transformer design was chosen is that the transmission line design is similar to the taper design of the

previous project, and exponential transmission line transformers can operate at high frequencies at an ultra-wide bandwidth. Extensive work has been done in the past with exponential transmission line transformers using square pulses as well [18,46].

The main concept behind the exponential line design is in the relationship that impedance discontinuities have with the wavelengths of the transmitted pulse. An exponential line transformer operates on a wideband and can be thought of as a form of high pass filter [47]. In this transformer design, very low frequencies, with high wavelengths, are the most to be attenuated. In addition, faster impedance shifting will result in a higher pass filter, and so only lower wavelengths can pass without significant attenuation. The effect of the increase in impedance is based on the percentage increase of the impedance. Transformer starting at 50-Ω, an increase of 5-Ω will have the same wavelengths requirements as a transformer starting at a lower 10-Ω and only increasing by 1-Ω, so long as the impedance changes are done across the same distance. A rule of thumb used in the design of exponential transformers is that a frequency with a wavelength *x* can only be properly transmitted as long as the impedance shifts significantly less than 60% along that same length *x*.

The transformer can be seen as more ‘sensitive’ at its port with lower impedance. The ideal way to increase impedance across its length, such that the percentage increase of impedance is constant, would be an exponential shift. This

exponential shift of the impedance can be translated into an exponential shift in the dimensions of the active plane on the transmission line transformer.

The dielectric material is more important than before as well for this transformer. As the speed of the transmitted pulse is directly impacted by the dielectric constant of the material, a dielectric with a higher constant, and therefore lower transmission speed, will have smaller wavelengths for the same frequency. Smaller wavelengths mean better transmission, as the impedance will not be shifting as 'quickly'. A higher dielectric constant will positively impact the performance of the transformer. The RO3010 material is perfect as it has a high dielectric constant.

With a pulse length of 1 picosecond across this transformer, simulations estimate approximately 90% transmission. Once the transformer is fabricated using copper etching, the coaxial element will be attached through soldering. Testing within the suitcase is still to be done.

CHAPTER 5
CONCLUSION

Transmission line pulse transformers are useful in operation because of their simplicity in design. These designs are reciprocal networks, they have no moving parts, and do not require the use of diodes or semiconductors. These factors allow for a high degree of flexibility when fabricating and implementing these transformers. Fabrication in particular can be done cheaply and efficiently, using common dielectric materials and simple shaping processes. There is no need for highly complex materials or designs, as these transformers operate solely on the principles of transmission lines and impedance shifting. These transformers additionally can operate on an ultra-wide bandwidth and have no issues with high power transmission, as long as the dielectric material has a high enough dielectric strength.

At the same time, transmission line pulse transformers are very sensitive to faults in their design. These transformers will react very negatively to small impedance discontinuities, and it is important that precise measurements are made to ensure the correct impedance at all points across the transformer's length. While these designs are simple, they must be precise and exact.

As for purposes where operation on a high frequency bandwidth is not a requirement, it may be better to use alternate transformer types. Other designs, such as inverting transformers and two-stage voltage transformers, can transmit

pulses across through changing geometries and impedance, often with better less losses, but over a smaller bandwidth.

As for when it is required to have a high-power, high bandwidth pulse transformer, the transmission line transformer is a quality and accessible option. The nature of the device allows for implementing features such as shielding without affecting the transmission.

BIBLIOGRAPHY

[1] W. Wiesbeck and L. Sit, "Radar 2020: The future of radar systems," 2014 International Radar Conference, Lille, 2014, pp. 1-6, doi: 10.1109/RADAR.2014.7060395.

[2] G. Wu et al., "Design and Experimental Measurement of Input and Output Couplers for a 6–18-GHz High-Power Helix Traveling Wave Tube Amplifier," in IEEE Transactions on Electron Devices, vol. 67, no. 4, pp. 1826-1831, April 2020, doi: 10.1109/TED.2020.2975645.

[3] [3]B. A. Kumar and P. T. Rao, "Overview of advances in communication technologies," 2015 13th International Conference on Electromagnetic Interference and Compatibility (INCEMIC), Visakhapatnam, 2015, pp. 102-106, doi: 10.1109/INCEMIC.2015.8055856

[4] R. J. Mailloux, "Antenna array architecture," in Proceedings of the IEEE, vol. 80, no. 1, pp. 163-172, Jan. 1992, doi: 10.1109/5.119575.

[5] R. C. Heimiller, J. E. Belyea and P. G. Tomlinson, "Distributed Array Radar," in IEEE Transactions on Aerospace and Electronic Systems, vol. AES-19, no. 6, pp. 831-839, Nov. 1983, doi: 10.1109/TAES.1983.309395.

[6] Mitha, T., Pour, M. Principles of adaptive element spacing in linear array antennas. Sci Rep 11, 5584 (2021). https://doi-org.proxy.library.umkc.edu/10.1038/s41598-021-84874-7

[7] G. Wheeler, "Broadband waveguide-to-coax transitions," 1958 IRE International Convention Record, New York, NY, USA, 1957, pp. 182-185, doi: 10.1109/IRECON.1957.1150581.

[8] M. Pardalopoulou and K. Solbach, "Over-moded operation of waveguide-to-coax transition at 60 GHz," Infrared and Millimeter Waves, Conference Digest of the 2004 Joint 29th International Conference on 2004 and 12th International Conference on Terahertz Electronics, 2004., Karlsruhe, Germany, 2004, pp. 475-476, doi: 10.1109/ICIMW.2004.1422170.

[9] G. K. C. Kwan and N. K. Das, "Coaxial-probe to parallel-plate dielectric waveguide transition: analysis and experiment," 1998 IEEE MTT-S International Microwave Symposium Digest (Cat. No.98CH36192), Baltimore, MD, USA, 1998, pp. 245-248 vol.1, doi: 10.1109/MWSYM.1998.689366.W.-K. Chen, Linear Networks and Systems. Belmont, CA, USA: Wadsworth, 1993, pp. 123–135.

[10] Kwan, G.K.C. & Das, Nirod. (2002). Excitation of a parallel-plate dielectric waveguide using a coaxial probe - Basic characteristics and experiments. Microwave Theory and Techniques, IEEE Transactions on. 50. 1609 - 1620. 10.1109/TMTT.2002.1006423.

[11] I. Fabregas, K. Shamsaifar and J. M. Rebollar, "Coaxial to rectangular waveguide transitions," IEEE Antennas and Propagation Society International Symposium 1992 Digest, Chicago, IL, USA, 1992, pp. 2122-2125 vol.4, doi: 10.1109/APS.1992.221447.

[12] S. Kawakami, "Lossless Reciprocal Transformation and Synthesis of a Two-State Network," in IEEE Transactions on Circuit Theory, vol. 13, no. 2, pp. 128-136, June 1966, doi: 10.1109/TCT.1966.1082584.

[13] Longfang Ye, Ruimin Xu, Zhihui Wang, and Weigan Lin, "A novel broadband coaxial probe to parallel plate dielectric waveguide transition at THz frequency," Opt. Express 18, 21725-21731 (2010)

[14] W. Yi, E. Li, G. Guo and R. Nie, "An X-band coaxial-to-rectangular waveguide transition," 2011 IEEE International Conference on Microwave Technology & Computational Electromagnetics, Beijing, China, 2011, pp. 129-131, doi: 10.1109/ICMTCE.2011.5915181.

[15] L. Solymar, "Some Notes on the Optimum Design of Stepped Transmission-Line Transformers," in IRE Transactions on Microwave Theory and Techniques, vol. 6, no. 4, pp. 374-378, October 1958, doi: 10.1109/TMTT.1958.1125208.

[16] V. P. Meschanov, I. A. Rasukova and V. D. Tupikin, "Stepped transformers on TEM-transmission lines," in IEEE Transactions on Microwave Theory and Techniques, vol. 44, no. 6, pp. 793-798, June 1996, doi: 10.1109/22.506436.

[17] K. Vinayagamoorthy, J. Coetzee and D. Jayalath, "Microstrip to Parallel Strip Balun as Spiral Antenna Feed," 2012 IEEE 75th Vehicular Technology Conference (VTC Spring), 2012, pp. 1-5, doi: 10.1109/VETECS.2012.6240118.

[18] Paul. W. Smith “Transient Electronics – Pulsed Circuit Technology” Wiley, 2002

[19] A. O. Bah, Pei-Yuan Qin and Y. J. Guo, "An extremely wideband tapered balun for application in tightly coupled arrays," 2016 IEEE-APS Topical Conference on Antennas and Propagation in Wireless Communications (APWC), 2016, pp. 162-165, doi: 10.1109/APWC.2016.7738146.

[20] P. L. Carro, J. de Mingo, P. García-Dúcar and C. Sanchez, "Synthesis of Hecken-tapered microstrip to Paralell-Strip baluns for UHF frequency band," 2011 IEEE MTT-S International Microwave Symposium, 2011, pp. 1-4, doi: 10.1109/MWSYM.2011.5972676.

[21] J. W. Duncan and V. P. Minerva, "100:1 Bandwidth Balun Transformer," in Proceedings of the IRE, vol. 48, no. 2, pp. 156-164, Feb. 1960, doi: 10.1109/JRPROC.1960.287458.

[22] X. Chen, Z. Zhang, S. Yu and T. Zsurzsan, "Fringing Effect Analysis of Parallel Plate Capacitors for Capacitive Power Transfer Application," 2019 IEEE 4th International Future Energy Electronics Conference (IFEEC), Singapore, Singapore, 2019, pp. 1-5, doi: 10.1109/IFEEC47410.2019.9015111.

[23] W. A. Johnson, L. X. Schneider and E. L. Neau, "Theory, simulation, and experiment of a single module coax-to-parallel-plate transition for the transformer section of pbfa II," 7th Pulsed Power Conference, Monterey, CA, USA, 1989, pp. 54-57, doi: 10.1109/PPC.1989.767420.

[24] M. N. O. Sadiku, "A simple introduction to finite element analysis of electromagnetic problems," in IEEE Transactions on Education, vol. 32, no. 2, pp. 85-93, May 1989, doi: 10.1109/13.28037.

[25] S. Uatrongjit, J. Vilasdechanon and K. Likit-Anurucks, "Finite difference method for steady state analysis of nonlinear circuit with distributed elements," IEEE APCCAS 2000. 2000 IEEE Asia-Pacific Conference on Circuits and Systems. Electronic Communication Systems. (Cat. No.00EX394), Tianjin, China, 2000, pp. 219-222, doi: 10.1109/APCCAS.2000.913447.

[26] .Altair FEKO CADFEKO version 2019 0.1-349439

[27] COMSOL Multiphysics® v. 5.4. www.comsol.com. COMSOL AB, Stockholm, Sweden

[28] ATCL2 v1.04, http://www.hdtvprimer.com/kq6qv/atlc2.html, Dr. David Kirkby, G8WRB

[29] Autodesk.co.uk. 2018. Cloud Powered 3D CAD/CAM Software for Product Design | Fusion 360. [online] Available at: <https://www.autodesk.co.uk/products/fusion-360/overview?referrer=%2Fproducts%2Ffusion-360%2Foverview> [Accessed 28 January 2018].

[30] J. Martens, D. Judge and J. Bigelow, "Multiport vector network analyzer measurements," in IEEE Microwave Magazine, vol. 6, no. 4, pp. 72-81, Dec. 2005, doi: 10.1109/MMW.2005.1580339.

[31] D. Antonovici, "Advances in Time Domain Reflectometry characterisation for high speed interconnects," 2015 IEEE 21st International Symposium for Design and Technology in Electronic

Packaging (SIITME), Brasov, Romania, 2015, pp. 37-40, doi: 10.1109/SIITME.2015.7342291.

[32] S. K. Sharma, P. Deb, A. Sharma and A. Shyam, "Development of compact pulse forming lines using higher dielectric constant mediums," 2014 International Symposium on Discharges and Electrical Insulation in Vacuum (ISDEIV), Mumbai, India, 2014, pp. 349-351, doi: 10.1109/DEIV.2014.6961691.

[33] L. Mandelcorn, R. E. Hoff and G. R. Sprengling, "The effects of electrical discharges between electrodes across insulation surfaces II. Discharges occurring in static air," Annual Report 1960 Conference on Electrical Insulation, Washington, DC, USA, 1960, pp. 115-121, doi: 10.1109/CEI.1960.7461677.

[34] P. G. Slade and E. D. Taylor, "Electrical breakdown in atmospheric air between closely spaced (0.2 /spl mu/m-40 /spl mu/m) electrical contacts," Proceedings of the Forth-Seventh IEEE Holm Conference on Electrical Contacts (IEEE Cat. No.01CH37192), Montreal, QC, Canada, 2001, pp. 245-250, doi: 10.1109/HOLM.2001.953218.

[35] T. Yamashita et al., "Estimation of surface breakdown voltage of solid/gas composite insulation with embedded electrode," in IEEE Transactions on Dielectrics and Electrical Insulation, vol. 23, no. 5, pp. 3026-3033, October 2016, doi: 10.1109/TDEI.2016.7736866.

[36] O. C. Feet, F. Mauseth and K. Niayesh, "Influence of Surface Roughness on Breakdown in Air Gaps at Atmospheric Pressure Under Lightning Impulse," 2018 IEEE International Conference on High Voltage Engineering and Application (ICHVE), Athens, Greece, 2018, pp. 1-4, doi: 10.1109/ICHVE.2018.8642269.

[37] W. V. Houston, "The theory of electrical conductivity recent developments," in Journal of the A.I.E.E., vol. 48, no. 11, pp. 795-799, Nov. 1929, doi: 10.1109/JAIEE.1929.6535938.

[38] H. A. Wheeler, "Formulas for the Skin Effect," in Proceedings of the IRE, vol. 30, no. 9, pp. 412-424, Sept. 1942, doi: 10.1109/JRPROC.1942.232015.

[39] Dimuthu Wanasinghe, Farhad Aslani, “A review on recent advancement of electromagnetic interference shielding novel metallic materials and processes”, Composites Part B: Engineering, Volume 176, 2019

[40] P. Koch et al., "Development of copper etch technology for advanced copper interconnects," 10th Annual IEEE/SEMI. Advanced

Semiconductor Manufacturing Conference and Workshop. ASMC 99 Proceedings (Cat. No.99CH36295), Boston, MA, USA, 1999, pp. 290-294, doi: 10.1109/ASMC.1999.798247.

[41] K. Ganesan et al., "Innovative Advances in Copper Electroplating for IC Substrate Manufacturing," 2017 IEEE 67th Electronic Components and Technology Conference (ECTC), Orlando, FL, USA, 2017, pp. 1369-1377, doi: 10.1109/ECTC.2017.87.

[42] C. E. Baum and J. M. Lehr, "Tapered transmission-line transformers for fast high-voltage transients," in IEEE Transactions on Plasma Science, vol. 30, no. 5, pp. 1712-1721, Oct. 2002, doi: 10.1109/TPS.2002.806614.

[43] J. Kolodzey et al., "Electrical conduction and dielectric breakdown in aluminum oxide insulators on silicon," in IEEE Transactions on Electron Devices, vol. 47, no. 1, pp. 121-128, Jan. 2000, doi: 10.1109/16.817577.

[44] Z. Junru, Z. Wensi, Y. Mengxia and W. Yuanyuan, "Design of ultra wide band transition connector for GTEM cell," 2011 International Conference on Electronics, Communications and Control (ICECC), Ningbo, 2011, pp. 3657-3660, doi: 10.1109/ICECC.2011.6066569.

[45] M. L. Crawford, "Generation of Standard EM Fields Using TEM Transmission Cells," in IEEE Transactions on Electromagnetic Compatibility, vol. EMC-16, no. 4, pp. 189-195, Nov. 1974, doi: 10.1109/TEMC.1974.303364.

[46] R. N. Ghose, "Exponential Transmission Lines as Resonators and Transformers," in IRE Transactions on Microwave Theory and Techniques, vol. 5, no. 3, pp. 213-217, July 1957, doi: 10.1109/TMTT.1957.1125143.

[47] P. LaTourrette, "High Pass Filter Design," 1982 12th European Microwave Conference, Helsinki, Finland, 1982, pp. 233-238, doi: 10.1109/EUMA.1982.333169.

VITA

James Kovarik was born in Phoenix, Arizona on March 7th, 1997. He was educated at Veritas Preparatory Academy, a local charter school. He obtained a Bachelor of Science in engineering from Rockhurst University. He is currently a graduate student at the University of Missouri in Kansas City. He is studying electrical engineering and works as a research assistant under Anthony Caruso. His research focuses on electric field theory and he plans to graduate in 2021.